

Multi-terminal nonreciprocal routing in an optomechanical plaquette via synthetic magnetism

Zhi-Xiang Tang and Xun-Wei Xu*

*Key Laboratory of Low-Dimensional Quantum Structures and Quantum Control of Ministry of Education,
Key Laboratory for Matter Microstructure and Function of Hunan Province,
Department of Physics and Synergetic Innovation Center for Quantum Effects and Applications,
Hunan Normal University, Changsha 410081, China*

(Dated: August 30, 2023)

Optomechanical systems with parametric coupling between optical (photon) and mechanical (phonon) modes provide a useful platform to realize various magnetic-free nonreciprocal devices, such as isolators, circulators, and directional amplifiers. However, nonreciprocal router with multi-access channels has not been extensively studied yet. Here, we propose a nonreciprocal router with one transmitter, one receiver, and two output terminals, based on an optomechanical plaquette composing of two optical modes and two mechanical modes. The time-reversal symmetry of the system is broken via synthetic magnetism induced by driving the two optical modes with phase-correlated laser fields. The prerequisites for nonreciprocal routing are obtained both analytically and numerically, and the robustness of the nonreciprocity is demonstrated numerically. Multi-terminal nonreciprocal router in optomechanical plaquette provides a useful quantum node for development of quantum network information security and realization of quantum secure communication.

I. INTRODUCTION

In a linear magnetic-free system, the transport of light is governed by the Lorentz reciprocity theorem [1, 2]. Nevertheless, nonreciprocal optical devices are the basic building blocks for information processing and sensing [3, 4], so we need to break the time-reversal symmetry of the system. Recently, in order to satisfy the demand of on-chip integrated information processing, the research of magnetic-free optical nonreciprocity scheme has attracted a lot of attention. As one of the most promising magnetic-free nonreciprocal schemes, optomechanically induced nonreciprocity has attracted much interest in the past decade [5–7], and various nonreciprocal mechanisms are proposed theoretically and demonstrated experimentally based on optomechanical interactions, such as direction-dependent optomechanical nonlinearity driven [8–11], microring with unidirectional pumping [12–18], stimulated Brillouin scattering [19, 20], dynamically encircling an exceptional point [21–23], Sagnac effect in spinning resonator [24–31], and quantum interference based on synthetic magnetism [32–34].

Optomechanical plaquette formed from the synthetic dimension created by the cycle coupling of optical and mechanical modes provides a ideal platform for nonreciprocity via synthetic flux threading the plaquette. Based on this plaquette, various nonreciprocal devices have been demonstrated, including optical isolator and circulator [34–38], nonreciprocal frequency converter [39], directional optical amplifier [40–43], nonreciprocal ground-state cooling [44–46], asymmetric optomechanical entanglement [47], and such structure has been extended to optomechanical arrays to realize nonreciprocal control of phonon flow [48–50] and simulate

gauge fields in many-body physics [51–53]. Similar mechanisms have been realized for optical photons in optomechanical crystals [54–56] and microresonators [57], and microwave photons in superconducting circuits [58–62].

Router for controlling the path of signals, is a key element in constructing network, and has been carried out in multi-waveguides connected by atoms [63–68], QED systems [69–72], or optomechanical systems [73–75], and one bus-waveguide side coupled to numerous quantum emitters [76–78]. For the further development of quantum network information security and the realization of quantum secure communication, nonreciprocal router that steers the signals transport in one direction deserves more exploration. Although the nonreciprocal routers with only one output terminal have been proposed theoretically [79–82] and realized experimentally in optomechanics [83], nonreciprocal routing with multiaccess channels has not been extensively studied yet.

In this paper, we introduce a nonreciprocal router with one transmitter, one receiver, and two output terminals, and propose a scheme to realized the nonreciprocal router based on an optomechanical plaquette composing of two optical modes and two mechanical modes. We demonstrate that the optomechanical plaquette can serve as a nonreciprocal router with one optical mode as transmitter, another optical mode as receiver, and two mechanical modes as output terminals. We will investigate the optimal conditions for nonreciprocal router and discuss its robustness against the imperfectness. Our work may inspire the study of nonreciprocal quantum nodes for scalable quantum information processing in quantum secure network and communication.

The remainder of the paper is organized as follows. In Sec. II, we introduces the model of nonreciprocal router and show how to realize it in an optomechanical plaquette. In Sec. III, we show the nonreciprocal scattering matrix of the optomechanical plaquette and discusses the

* xwxu@hunnu.edu.cn

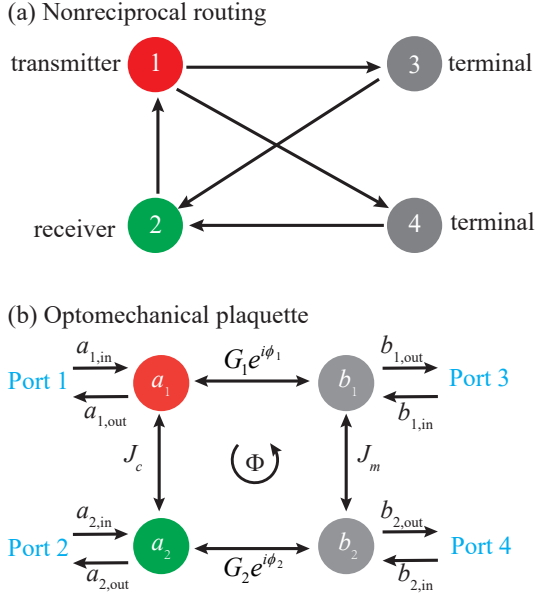


FIG. 1. (Color online) (a) Schematic diagram of a nonreciprocal router with one transmitter, one receiver, and two output terminals. The signals transport unidirectionally from the transmitter to the two terminals, from the terminals to the receiver, and from the receiver to the transmitter. (b) Schematic diagram of a four-mode optomechanical plaquette comprising of two optical modes (a_1 and a_2) and two mechanical modes (b_1 and b_2). The optical (mechanical) modes are coupled to each other with strength J_c (J_m), and the optical and mechanical modes (a_1 and b_1 , a_2 and b_2) are coupled via radiation pressure with the linearized optomechanical coupling strengths $G_1e^{i\phi_1}$ and $G_2e^{i\phi_2}$ and a synthetic flux $\Phi = \phi_2 - \phi_1$ threading the four-mode plaquette.

influence of experimental parameters on the nonreciprocal routing effect. This work is summarized in Sec. IV.

II. NONRECIPROCAL ROUTER AND OPTOMECHANICAL PLAQUETTE

In this section, we will introduce the basic ideal of a nonreciprocal router, and then propose an optomechanical model to realize the nonreciprocal router.

A. Nonreciprocal router

We consider a nonreciprocal router consisting of one transmitter, one receiver, and two terminals. The basic ideal for the nonreciprocal router considered in the paper is shown in Fig. 1(a). Let's introduce the characteristics of the nonreciprocal router. The nonreciprocity indicates that the signals transport nonreciprocal between different ports, which are shown in the following three aspects: Firstly, the nonreciprocity between the transmitter and the receiver is manifested as the signal can only be transmitted from the receiver to the transmit-

ter but not from the transmitter to the receiver. Secondly, the signal is transmitted from the transmitter to the terminals but cannot return from the terminals to the transmitter. Thirdly, the signal from the terminals can be transmitted to the receiver, but the signal from the receiver cannot transport to the terminals. In order to realize such functions in an integrated platform, we consider an optomechanical plaquette, which has been used to realize non-reciprocal photon transport with high isolation and directional optical amplification via synthetic magnetism [54–62].

B. Optomechanical plaquette

We consider an optomechanical plaquette composing of two optical modes a_j ($j = 1, 2$) with frequency $\omega_{c,j}$ and two mechanical modes b_j with frequency ω_j , as shown in Fig. 1(b). The two optical (mechanical) modes couple to each other with strength J_c (J_m), and the optical mode (a_j) interacts with the mechanical mode (b_j) via radiation pressure with single-photon optomechanical coupling rate g_j . To enhance the optomechanical coupling strength g_j , each optical mode is pumped by a strong optical field with strength ε_j and frequency $\omega_{p,j}$ relatively detuned from the resonant frequency of optical mode $\omega_{c,j}$ by the mechanical frequency ω_j , $\Delta_{0,j} \equiv \omega_{c,j} - \omega_{p,j} \approx \omega_j$. In a rotating frame with respect to the unitary transformation $R(t) = \exp(-i \sum_{j=1,2} \omega_{p,j} t a_j^\dagger a_j)$, the optomechanical plaquette can be described by a Hamiltonian as ($\hbar = 1$)

$$\begin{aligned}
 H = & \sum_{j=1,2} \left[\Delta_{0,j} a_j^\dagger a_j + \omega_j b_j^\dagger b_j + g_j a_j^\dagger a_j (b_j^\dagger + b_j) \right] \\
 & + J_c (a_1^\dagger a_2 + a_1 a_2^\dagger) + J_m (b_1^\dagger b_2 + b_1 b_2^\dagger) \\
 & + i (\varepsilon_1 a_1 e^{i\varphi_1} + \varepsilon_2 a_2 e^{i\varphi_2} - \text{H.c.}), \quad (1)
 \end{aligned}$$

where φ_1 and φ_2 are the phases of the pumping fields and they are correlated, as an essential ingredient for nonreciprocity.

According to the Heisenberg equation of motion and taking into account the damping and corresponding input noise, we get the quantum Langevin equations (QLEs) as

$$\begin{aligned}
 \frac{d}{dt} a_1 = & \left\{ -\frac{\kappa}{2} - i \left[\Delta_{0,1} + g_1 (b_1^\dagger + b_1) \right] \right\} a_1 \\
 & - i J_c a_2 - \varepsilon_1 e^{-i\varphi_1} + \sqrt{\kappa_e} a_{1,\text{in}} + \sqrt{\kappa_0} a_{1,\text{vac}}, \quad (2)
 \end{aligned}$$

$$\begin{aligned}
 \frac{d}{dt} a_2 = & \left\{ -\frac{\kappa}{2} - i \left[\Delta_{0,2} + g_2 (b_2^\dagger + b_2) \right] \right\} a_2 \\
 & - i J_c a_1 - \varepsilon_2 e^{-i\varphi_2} + \sqrt{\kappa_e} a_{2,\text{in}} + \sqrt{\kappa_0} a_{2,\text{vac}}, \quad (3)
 \end{aligned}$$

$$\begin{aligned}
 \frac{d}{dt} b_1 = & \left(-\frac{\gamma}{2} - i\omega_1 \right) b_1 - i g_1 a_1^\dagger a_1 \\
 & - i J_m b_2 + \sqrt{\gamma_e} b_{1,\text{in}} + \sqrt{\gamma_0} b_{1,\text{th}}, \quad (4)
 \end{aligned}$$

$$\begin{aligned} \frac{d}{dt}b_2 &= \left(-\frac{\gamma}{2} - i\omega_2\right)b_2 - ig_2a_2^\dagger a_2 \\ &\quad - iJ_m b_1 + \sqrt{\gamma_e}b_{2,\text{in}} + \sqrt{\gamma_0}b_{2,\text{th}}, \end{aligned} \quad (5)$$

where κ_e and κ_0 (γ_e and γ_0) are the external and internal decay rates of optical (mechanical) modes, with the corresponding input optical fields $a_{j,\text{in}}$ and $a_{j,\text{vac}}$ (mechanical fields $b_{j,\text{in}}$ and $b_{j,\text{th}}$). $\kappa = \kappa_e + \kappa_0$ and $\gamma = \gamma_e + \gamma_0$ are the total decay rate of the optical and mechanical modes, respectively.

To obtain the linear response of the system to weak optical and mechanical signals, we will solve the QLEs by the standard process of the linearization [5]. We solve the QLEs in steady state based on the mean field approximation first, then the linearization of the system near the steady-state values yields to the corresponding linearized QLEs. The steady-state values $\alpha_j \equiv \langle a_j \rangle$ and $\beta_j \equiv \langle b_j \rangle$ are obtained from the QLEs by setting the time derivative terms to zero and using the factorization assumption $\langle AB \rangle = \langle A \rangle \langle B \rangle$ for any two operators A and B , as

$$\alpha_1 = e^{-i\varphi_1} \frac{\left(-\frac{\kappa}{2} - i\Delta_2\right)\varepsilon_1 + iJ_c\varepsilon_2 e^{-i(\varphi_2 - \varphi_1)}}{\left(-\frac{\kappa}{2} - i\Delta_2\right)\left(-\frac{\kappa}{2} - i\Delta_1\right) + J_c^2}, \quad (6)$$

$$\alpha_2 = e^{-i\varphi_2} \frac{\left(-\frac{\kappa}{2} - i\Delta_1\right)\varepsilon_2 + iJ_c\varepsilon_1 e^{i(\varphi_2 - \varphi_1)}}{\left(-\frac{\kappa}{2} - i\Delta_2\right)\left(-\frac{\kappa}{2} - i\Delta_1\right) + J_c^2}, \quad (7)$$

where $\Delta_j \equiv \Delta_{0,j} + g_j(\beta_j^* + \beta_j)$. Suppose $\varepsilon_1 \sim \varepsilon_2$ and $|\Delta_j| \gg J_c$, then we have

$$\alpha_j = |\alpha_j| e^{i\phi_j} \approx \frac{\varepsilon_j e^{-i\varphi_j}}{\left(-\frac{\kappa}{2} - i\Delta_j\right)}, \quad (8)$$

which means that the amplitude $|\alpha_j|$ and phase ϕ_j of α_j can be freely adjusted by the external field $\varepsilon_j e^{-i\varphi_j}$.

The linearized QLEs for the quantum fluctuation operators $\delta a_j \equiv a_j - \alpha_j$ and $\delta b_j \equiv b_j - \beta_j$ ($j = 1, 2$) are obtained as

$$\begin{aligned} \frac{d}{dt}\delta a_1 &= \left(-\frac{\kappa}{2} - i\Delta_1\right)\delta a_1 - iJ_c\delta a_2 - iG_1 e^{i\phi_1}\delta b_1 \\ &\quad + \sqrt{\kappa_e}a_{1,\text{in}} + \sqrt{\kappa_0}a_{1,\text{vac}}, \end{aligned} \quad (9)$$

$$\begin{aligned} \frac{d}{dt}\delta a_2 &= \left(-\frac{\kappa}{2} - i\Delta_2\right)\delta a_2 - iJ_c\delta a_1 - iG_2 e^{i\phi_2}\delta b_2 \\ &\quad + \sqrt{\kappa_e}a_{2,\text{in}} + \sqrt{\kappa_0}a_{L,\text{vac}}, \end{aligned} \quad (10)$$

$$\begin{aligned} \frac{d}{dt}\delta b_1 &= \left(-\frac{\gamma}{2} - i\omega_1\right)\delta b_1 - iJ_m\delta b_2 - iG_1 e^{-i\phi_1}\delta a_1 \\ &\quad + \sqrt{\gamma_e}b_{1,\text{in}} + \sqrt{\gamma_0}b_{1,\text{th}}, \end{aligned} \quad (11)$$

$$\begin{aligned} \frac{d}{dt}\delta b_2 &= \left(-\frac{\gamma}{2} - i\omega_2\right)\delta b_2 - iJ_m\delta b_1 - iG_2 e^{-i\phi_2}\delta a_2 \\ &\quad + \sqrt{\gamma_e}b_{2,\text{in}} + \sqrt{\gamma_0}b_{2,\text{th}}. \end{aligned} \quad (12)$$

Here $G_1 = |\alpha_1|g_1$ and $G_2 = |\alpha_2|g_2$ are the linearized optomechanical coupling strengths; the nonlinear terms are

negligible for the assumption $|\alpha_j|^2 \gg \langle \delta a_j^\dagger \delta a_j \rangle$, and the counter-rotating terms are neglected based on rotation-wave approximation under conditions $\Delta_j \approx \omega_j \gg G_j$.

The linearized QLEs can be concisely expressed as

$$\frac{d}{dt}V(t) = -MV(t) + \sqrt{\Gamma_e}V_{\text{in}}(t) + \sqrt{\Gamma_0}V_{\text{noise}}(t), \quad (13)$$

where $V(t)$ is the vector for the quantum fluctuation operators defined by $V(t) \equiv (\delta a_1, \delta a_2, \delta b_1, \delta b_2)^T$, $V_{\text{in}}(t) \equiv (a_{1,\text{in}}, a_{2,\text{in}}, b_{1,\text{in}}, b_{2,\text{in}})^T$, $V_{\text{noise}}(t) \equiv (a_{1,\text{vac}}, a_{2,\text{vac}}, b_{1,\text{th}}, b_{2,\text{th}})^T$, $\Gamma_e \equiv \text{diag}(\kappa_e, \kappa_e, \gamma_e, \gamma_e)$, $\Gamma_0 \equiv \text{diag}(\kappa_0, \kappa_0, \gamma_0, \gamma_0)$, and the linearized coefficient matrix M is given by

$$M = \begin{pmatrix} \frac{\kappa}{2} + i\Delta_1 & iJ_c & iG_1 e^{i\phi_1} & 0 \\ iJ_c & \frac{\kappa}{2} + i\Delta_2 & 0 & iG_2 e^{i\phi_2} \\ iG_1 e^{-i\phi_1} & 0 & \frac{\gamma}{2} + i\omega_1 & iJ_m \\ 0 & iG_2 e^{-i\phi_2} & iJ_m & \frac{\gamma}{2} + i\omega_2 \end{pmatrix}. \quad (14)$$

In order to ensure the stability of the system, we need to ensure that the real part of all eigenvalues of the coefficient matrix M are positive in the following discussions.

The linearized QLEs can be solved analytically in the frequency domain by the method of Fourier transform, with the definition of Fourier transform for operator o as

$$\tilde{o}(\omega) = \frac{1}{\sqrt{2\pi}} \int_{-\infty}^{+\infty} o(t) e^{i\omega t} dt. \quad (15)$$

The solution of the linearized QLEs in the frequency domain is obtained as

$$\tilde{V}(\omega) = (M - i\omega I)^{-1} \left[\sqrt{\Gamma_e} \tilde{V}_{\text{in}}(\omega) + \sqrt{\Gamma_0} \tilde{V}_{\text{noise}}(\omega) \right], \quad (16)$$

where I denotes the identity matrix. Based on the input-output relation [84]

$$\tilde{a}_{j,\text{out}}(\omega) + \tilde{a}_{j,\text{in}}(\omega) = \sqrt{\kappa_e} \tilde{\delta a}_j(\omega), \quad (17)$$

$$\tilde{b}_{j,\text{out}}(\omega) + \tilde{b}_{j,\text{in}}(\omega) = \sqrt{\gamma_e} \tilde{\delta b}_j(\omega), \quad (18)$$

the output fields from the optomechanical system are obtained as

$$\tilde{V}_{\text{out}}(\omega) = U(\omega) \tilde{V}_{\text{in}}(\omega) + W(\omega) \tilde{V}_{\text{noise}}(\omega), \quad (19)$$

where

$$U(\omega) = \sqrt{\Gamma_e} (M - i\omega I)^{-1} \sqrt{\Gamma_e} - I, \quad (20)$$

$$W(\omega) = \sqrt{\Gamma_e} (M - i\omega I)^{-1} \sqrt{\Gamma_0} \quad (21)$$

are the scattering matrices. So the scattering probabilities from Port j to Port i are given by

$$S_{ij}(\omega) = |U_{ij}(\omega)|^2, \quad (22)$$

where $U_{ij}(\omega)$ ($i, j = 1, 2, 3, 4$) denotes the element of $U(\omega)$ at i th row and j th column, given analytically in Appendix.

TABLE I. The inhibited scattering paths for different synthetic flux Φ and resonant frequency ω . The other parameters satisfy the conditions $\omega_m \gg \kappa = 2J_c \gg J_m \gg \gamma$, $G^2 = J_c\gamma \ll \kappa J_m$, where $\omega_1 = \omega_2 = \omega_m$, $\Delta_1 = \Delta_2 = \omega_m$, and $G_1 = G_2 = G$.

	$\omega = \omega_m - J_m$	$\omega = \omega_m + J_m$
$\Phi = \pi/2$	$S_{21}(\omega) \approx 0$	$S_{12}(\omega) \approx 0$
	$S_{13}(\omega) \approx S_{14}(\omega) \approx 0$	$S_{31}(\omega) \approx S_{41}(\omega) \approx 0$
	$S_{32}(\omega) \approx S_{42}(\omega) \approx 0$	$S_{23}(\omega) \approx S_{24}(\omega) \approx 0$
$\Phi = 3\pi/2$	$S_{12}(\omega) \approx 0$	$S_{21}(\omega) \approx 0$
	$S_{31}(\omega) \approx S_{41}(\omega) \approx 0$	$S_{13}(\omega) \approx S_{14}(\omega) \approx 0$
	$S_{23}(\omega) \approx S_{24}(\omega) \approx 0$	$S_{32}(\omega) \approx S_{42}(\omega) \approx 0$

C. Parameter conditions for nonreciprocal routing

The optomechanical plaquette can work as a nonreciprocal router with the two optical modes acting as the transmitter and receiver, and the two modes as two terminals. For example, we can use the optical mode a_1 as the transmitter, a_2 as the receiver, and the two mechanical modes b_1 and b_2 as two terminals. In order to realize the nonreciprocal router shown in Fig. 1(a), the scattering probabilities from Port 1 to 2, from Ports 3 and 4 to 1, and from Port 2 to 3 and 4, should be significantly inhibited, i.e., approximately equal to zero as

$$\begin{aligned} S_{21}(\omega) &\approx 0, \\ S_{13}(\omega) &\approx S_{14}(\omega) \approx 0, \\ S_{32}(\omega) &\approx S_{42}(\omega) \approx 0. \end{aligned} \quad (23)$$

Besides that, we can also use the optical mode a_2 as the transmitter, a_1 as the receiver, and the two mechanical modes as two terminals. Then the scattering probabilities from Port 2 to 1, from Ports 3 and 4 to 2, and from Port 1 to 3 and 4, should be significantly inhibited as

$$\begin{aligned} S_{12}(\omega) &\approx 0, \\ S_{31}(\omega) &\approx S_{41}(\omega) \approx 0, \\ S_{23}(\omega) &\approx S_{24}(\omega) \approx 0. \end{aligned} \quad (24)$$

The parameter conditions for these scattering probabilities given in Eqs. (23) and (24) can be derived from the analytical expression of $U_{ij}(\omega)$ given in Appendix.

Before the numerical simulation given in the next section, let us derive the parameters conditions for nonreciprocal router analytically based on some assumptions. Without loss of generality, here we set $\omega_1 = \omega_2 = \omega_m$, $\Delta_1 = \Delta_2 = \omega_m$, and $G_1 = G_2 = G$ for simplicity. Moreover, we introduce the synthetic flux (relative phase) $\Phi \equiv \phi_2 - \phi_1$ threading the four-mode plaquette to break time-reversal symmetry of the system, leading to nonreciprocal transport of signals between different ports. Based on the Eqs. (A.1)-(A.16), we find that the optomechanical plaquette can work as a nonreciprocal router with a_1 as the transmitter and a_2 as the receiver around the frequency $\omega = \omega_m - J_m$ for $\Phi = \pi/2$ or around the

frequency $\omega = \omega_m + J_m$ for $\Phi = 3\pi/2$. Conversely, the optomechanical plaquette can also work as a nonreciprocal router with a_1 as the receiver and a_2 as the transmitter around the frequency $\omega = \omega_m + J_m$ for $\Phi = \pi/2$ or around the frequency $\omega = \omega_m - J_m$ for $\Phi = 3\pi/2$. The other parameter conditions are given by:

(i) to realize $S_{12}(\omega) \approx 0$ or $S_{21}(\omega) \approx 0$, the parameters need to satisfy the conditions

$$J_m \gg \gamma, \quad G_1 = G_2 = \sqrt{J_c\gamma}; \quad (25)$$

(ii) $S_{14}(\omega) \approx S_{32}(\omega) \approx 0$ or $S_{41}(\omega) \approx S_{23}(\omega) \approx 0$, are expected with the parameters satisfying the conditions

$$\kappa \gg J_m \gg \gamma, \quad \kappa = 2J_c; \quad (26)$$

(iii) $S_{13}(\omega) \approx S_{42}(\omega) \approx 0$ or $S_{31}(\omega) \approx S_{24}(\omega) \approx 0$, are obtained under the conditions

$$\kappa \gg J_m \gg \gamma, \quad G^2 \ll \kappa J_m, \quad \kappa = 2J_c. \quad (27)$$

The conditions for nonreciprocal routing are summarized in Table I.

The conditions required to observe nonreciprocal routing can be reached for the current state-of-the-art optomechanical crystal circuit systems. For example, Ref. [54] demonstrated nonreciprocal photon transport and amplification by an optomechanical plaquette with the parameters: mechanical frequency $\omega_m/2\pi \approx 5.8$ GHz, external optical damping rate $\kappa_e/2\pi \approx 0.75 \sim 1$ GHz, intrinsic optical damping rate $\kappa_0/2\pi \approx 0.3$ GHz, single-photon optomechanical coupling rate $g_i/2\pi \approx 0.8$ MHz, mechanical dissipation rate $\gamma/2\pi \approx 4 \sim 5$ MHz, optical hopping rate $J_c/2\pi \approx 0.1 \sim 1.4$ GHz, mechanical hopping rate $J_m/2\pi \approx 2.8$ MHz. The coupling rates J_c and J_m can be varied by changing the number and shape of the holes that make up the optomechanical crystal between the two optomechanical cavities [85]. The linearized optomechanical coupling rates $G_j = |\alpha_j|g_j$ can be enhanced by pumping the optomechanical cavities with phase-correlated lasers.

III. NONRECIPROCAL ROUTING

In this section, we will show the nonreciprocal routing effect in the optomechanical plaquette by numerical calculations. As a simple example, we show the nonreciprocal scattering matrix first. Then, we discuss the optimal parameters (synthetic flux Φ , optomechanical coupling rate G , and external decay rate κ_e) for nonreciprocal routing, and the effects of the detuning between the two mechanical modes ($\delta = \omega_1 - \omega_2$) and internal optical and mechanical decays (κ_0 and γ_0) on nonreciprocal routing.

A. Nonreciprocal scattering matrix

The scattering probabilities $S_{ij}(\omega)$ between different ports are shown as functions of the frequency $(\omega - \omega_m)/\gamma$

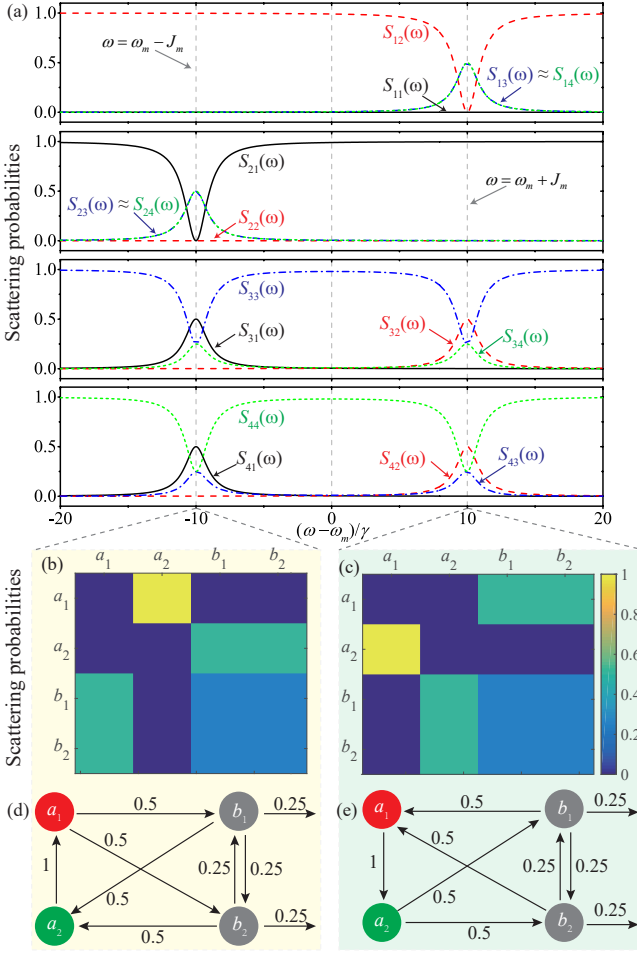


FIG. 2. (Color online) Scattering probabilities between different ports. (a) $S_{ij}(\omega)$ versus frequency $(\omega - \omega_m)/\gamma$. Scattering matrices for (b) $\omega = \omega_m - J_m$ and (c) $\omega = \omega_m + J_m$, with the corresponding probability flow charts given in (d) and (e), respectively. The parameters are $\omega_1 = \omega_2 = \omega_m$, $\Delta_1 = \Delta_2 = \omega_m$, $J_m = 10\gamma$, $J_c = 500\gamma$, $\gamma_0 = \kappa_0 = 0$, $\gamma_e = \gamma$, $\kappa_e = \kappa$, $\Phi = \pi/2$, $G_1 = G_2 = \sqrt{J_c\gamma}$, and $\kappa = 2J_c$.

in Fig. 2(a). The scattering probabilities $S_{ij}(\omega)$ change only round the splitting frequencies $\omega_m \pm J_m$ for the two mechanical modes $\omega_1 = \omega_2 = \omega_m$ with resonant interaction rate J_m . Specifically, at frequency $\omega = \omega_m - J_m$, the signals can transport from optical mode a_2 to a_1 with nearly one hundred percent probability, i.e., $S_{12}(\omega) \approx 1$; there is a 50/50 chance for the signals transport from a_1 either to b_1 or to b_2 , i.e., $S_{31}(\omega) \approx S_{41}(\omega) \approx 0.5$; the probability for the signals transport from b_1 or b_2 to a_2 is both about 50 percent, i.e., $S_{23}(\omega) \approx S_{24}(\omega) \approx 0.5$; all the transmission processes mentioned here are unidirectional, i.e., $S_{21}(\omega) \approx S_{14}(\omega) \approx S_{13}(\omega) \approx S_{42}(\omega) \approx S_{32}(\omega) \approx 0$. In other words, the optomechanical plaquette works as nonreciprocal router, with optical mode a_1 as transmitter, a_2 as receiver, and the two mechanical modes b_1 and b_2 as two terminals. In order to show the nonreciprocal routing behavior even more clearly, the scattering matrix for $\omega = \omega_m - J_m$ are shown in Fig. 2(b) and the

corresponding probability flow charts given in (d). It is obvious that the scattering matrix is asymmetry, and the probability flow are unidirectional.

In contrast, at frequency $\omega = \omega_m + J_m$, the optomechanical plaquette exhibits nonreciprocal routing behavior with signals transporting in different direction. As shown in Figs. 2(c) and 2(e), the optical mode a_2 is taken as a transmitter and the optical mode a_1 is taken as a receiver. As summarized in Table I, the optomechanical plaquette show nonreciprocal routing behavior in revers direction for $\Phi = \pi/2$ and $\Phi = 3\pi/2$. Thus we can steer the direction of the nonreciprocal routing by adjusting either the synthetic flux Φ or the frequency of the input signals.

B. Numerical results for optimal parameters

In order to understand the optimal conditions for non-reciprocal routing quantitatively, i.e., $\kappa = 2J_c$, $G = \sqrt{J_c\gamma}$, and $\Phi = \pi/2$ or $3\pi/2$, we show the scattering probabilities $S_{ij}(\omega)$ as functions of synthetic flux Φ , linearized optomechanical coupling strength G , and external optical decay κ_e in Figs. 3(a)-3(c) under the conditions $\omega_m \gg \kappa \gg J_m \gg \gamma$.

Synthetic flux Φ is one ingredient for breaking the time-reversal symmetry, and plays a key role in controlling the nonreciprocal routing [see Fig. 3(a)]. Agree with the analytical results given in Table I at frequency $\omega = \omega_m - J_m$, we have $S_{12}(\omega) \approx 1 \gg S_{21}(\omega)$ around $\Phi = \pi/2$ and $S_{12}(\omega) \ll S_{21}(\omega) \approx 1$ around $\Phi = 3\pi/2$. Similarly, we have $S_{31}(\omega) \approx S_{41}(\omega) \approx S_{23}(\omega) \approx S_{24}(\omega) \approx 0.5 \gg \{S_{13}(\omega), S_{14}(\omega), S_{32}(\omega), S_{42}(\omega)\}$ around $\Phi = \pi/2$ and $S_{13}(\omega) \approx S_{14}(\omega) \approx S_{32}(\omega) \approx S_{42}(\omega) \approx 0.5 \gg \{S_{31}(\omega), S_{41}(\omega), S_{23}(\omega), S_{24}(\omega)\}$ around $\Phi = 3\pi/2$. So we can steer the transmission direction of the signals in the optomechanical plaquette by tuning the synthetic flux Φ , which can be freely adjusted by the external pumping lasers given in Eq. (8).

The scattering probabilities between Port 1 and 2 [$S_{12}(\omega)/S_{21}(\omega)$] show different behaviors with the ones between other Ports [$S_{31}(\omega)/S_{13}(\omega)$, $S_{41}(\omega)/S_{14}(\omega)$, $S_{23}(\omega)/S_{32}(\omega)$, and $S_{24}(\omega)/S_{42}(\omega)$]. According to the analytical results given in Sec. II C, in order to realize $S_{12}(\omega) \approx 1 \gg S_{21}(\omega)$, one required condition is $G_1 = G_2 = G = \sqrt{J_c\gamma}$. This condition agrees well with the numerical results shown in Fig. 3(b) (up). There is a dip in $S_{21}(\omega)$ around the value of $G \approx 22.4\gamma \approx \sqrt{J_c\gamma}$, with $S_{12}(\omega) \approx 1$ for a wide range of G . In contrast, the isolations [$S_{31}(\omega)/S_{13}(\omega)$, $S_{41}(\omega)/S_{14}(\omega)$, $S_{23}(\omega)/S_{32}(\omega)$, and $S_{24}(\omega)/S_{42}(\omega)$] decrease with the increasing of G . Nevertheless, we can obtain the maximal values of $S_{31}(\omega) \approx S_{41}(\omega) \approx S_{23}(\omega) \approx S_{24}(\omega) \approx 0.5$ under the condition $G \approx \sqrt{J_c\gamma}$ [see Fig. 3(b) (middle and down)].

As shown in Fig. 3(c) (middle and down), there is a dip for $\{S_{13}(\omega), S_{14}(\omega), S_{32}(\omega), S_{42}(\omega)\}$ with $S_{31}(\omega)$, $S_{41}(\omega)$, $S_{23}(\omega)$, and $S_{24}(\omega)$ reaching the maximal value

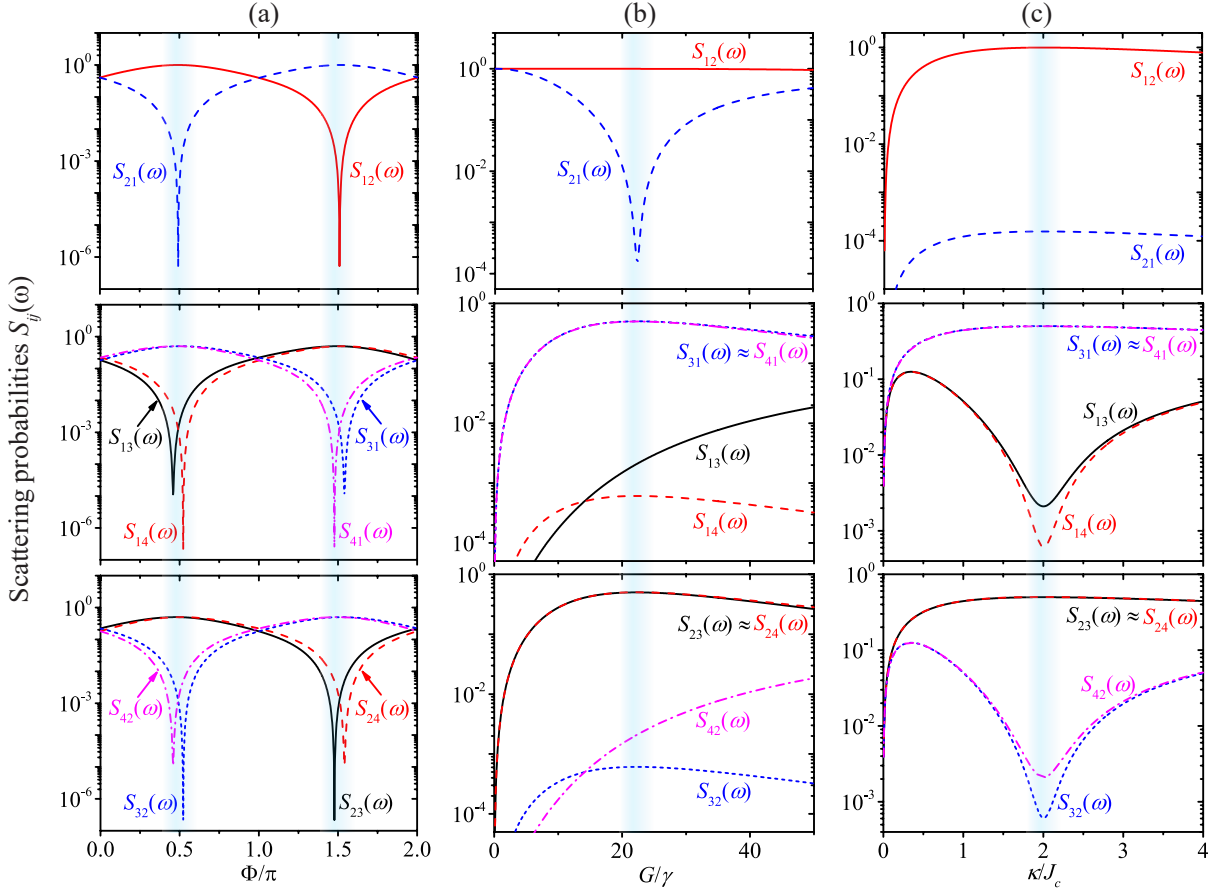


FIG. 3. (Color online) The optimal parameters for nonreciprocal routing. Scattering probabilities $S_{ij}(\omega)$ are plotted as functions of (a) the synthetic flux Φ/π for $\kappa = 2J_c$ and $G_1 = G_2 = \sqrt{J_c\gamma}$, (b) the optomechanical coupling strength $G_1 = G_2 \equiv G$ for $\Phi = \pi/2$ and $\kappa = 2J_c$, and (c) the optical decay rate κ/J_c for $\Phi = \pi/2$ and $G_1 = G_2 = \sqrt{J_c\gamma}$. The parameters are $\omega_1 = \omega_2 = \omega_m$, $\Delta_1 = \Delta_2 = \omega_m$, $J_m = 10\gamma$, $J_c = 500\gamma$, $\omega = \omega_m - J_m$, $\gamma_0 = \kappa_0 = 0$, $\gamma_e = \gamma$, and $\kappa_e = \kappa$.

0.5 around the point $\kappa \approx 2J_c$. These agree well with the required condition obtained analytically in Sec. II C. Differently, both $S_{12}(\omega)$ and $S_{21}(\omega)$ increase with the creasing of κ/J_c and reach the maximal value around the point $\kappa \approx 2J_c$, and the isolation $S_{12}(\omega)/S_{21}(\omega)$ is not sensitive to the change of κ/J_c [see Fig. 3(c) (up)].

C. Effects of detuning and internal decays

In the discussions above, we assume that the two mechanical modes have the same resonant frequency $\omega_1 = \omega_2 = \omega_m$ and ignore the intrinsic decay $\kappa_0 = \gamma_0 = 0$ for simplicity. However, there are unpredictable uncertainty in devices fabrication and we may have the frequency difference of two mechanical modes $\delta = \omega_1 - \omega_2$ and intrinsic decay κ_0 and γ_0 in experiments. In this subsection, we will show numerically that the nonreciprocal routing is robust against the mechanical frequency difference δ and intrinsic decay κ_0 and γ_0 .

The scattering probabilities are plotted as functions of the mechanical frequency difference δ/γ in Fig. 4(a).

$S_{21}(\omega)$ is sensitive to the mechanical frequency difference δ/γ , but $S_{12}(\omega)$ is almost unchanged. The isolation of $S_{12}(\omega)/S_{21}(\omega)$ decrease from 38dB to 10.2dB with the increasing of δ from 0 to $\pm 5\gamma$. The isolations of $S_{41}(\omega)/S_{14}(\omega)$, $S_{31}(\omega)/S_{13}(\omega)$, $S_{23}(\omega)/S_{32}(\omega)$, and $S_{24}(\omega)/S_{42}(\omega)$ are about 16dB at the mechanical frequency difference $\delta = \pm 5\gamma$.

In order to study the effect of the intrinsic optical decay on the nonreciprocal routing, the scattering probabilities are plotted as functions of κ_0/κ_e in Fig. 4(b). Both $S_{12}(\omega)$ and $S_{21}(\omega)$ decrease with the creasing of κ_0 , but the isolation of $S_{12}(\omega)/S_{21}(\omega)$ is not sensitive to the change of κ_0 [see Fig. 4(b) (up)]. The isolations of $S_{41}(\omega)/S_{14}(\omega)$, $S_{31}(\omega)/S_{13}(\omega)$, $S_{23}(\omega)/S_{32}(\omega)$, and $S_{24}(\omega)/S_{42}(\omega)$ decrease with the increasing of κ_0 , and reach about 9.4dB with intrinsic decay $\kappa_0 = \kappa_e$.

The effect of the intrinsic mechanical decay on the nonreciprocal routing is shown in Fig. 4(c). The scattering probability $S_{21}(\omega)$ increases with the creasing of γ_0 , and the isolation of $S_{12}(\omega)/S_{21}(\omega)$ decreases from 38dB to 9.5dB with the increasing of γ_0 from 0 to γ_e . In contrast, $S_{31}(\omega) \approx S_{41}(\omega)$ and $S_{23}(\omega) \approx S_{24}(\omega)$ decrease slowly

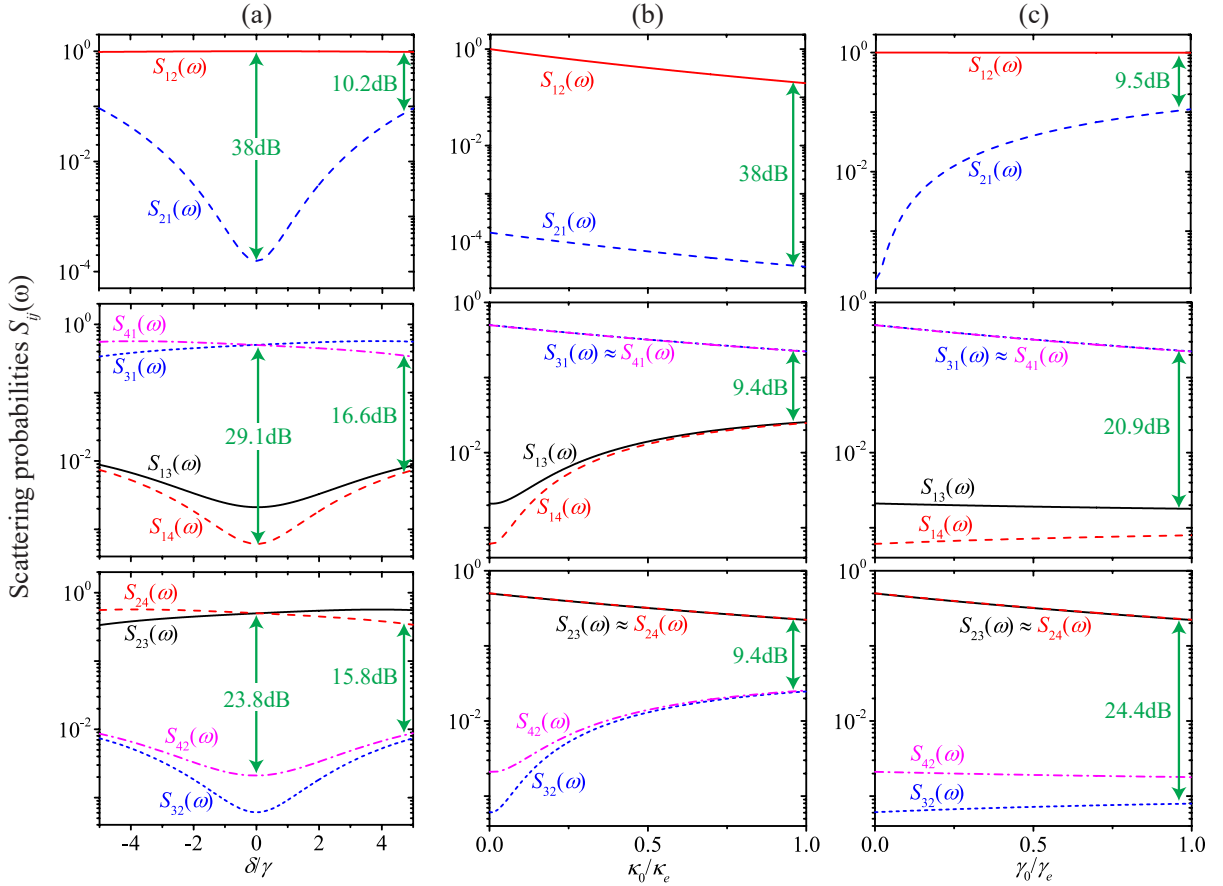


FIG. 4. (Color online) Effects of frequency difference and intrinsic decay on the nonreciprocal routing. Scattering probabilities $S_{ij}(\omega)$ are plotted as functions of (a) the frequency difference of two mechanical modes $\delta = \omega_1 - \omega_2$ for $\kappa_0 = \gamma_0 = 0$, (b) the intrinsic optical decay κ_0/κ_e for $\delta = \gamma_0 = 0$, and (c) the intrinsic mechanical decay γ_0/γ_e for $\delta = \kappa_0 = 0$. The parameters are $\omega_m = (\omega_1 + \omega_2)/2$, $\Delta_1 = \Delta_2 = \omega_m$, $\Phi = \pi/2$, $J_m = 10\gamma_e$, $J_c = 500\gamma_e$, $\kappa_e = 2J_c$, $G_1 = G_2 = \sqrt{J_c\gamma_e}$, and $\omega = \omega_m - J_m$.

with the increasing of γ_0 , and $S_{13}(\omega)$, $S_{14}(\omega)$, $S_{42}(\omega)$, and $S_{32}(\omega)$ are not sensitive to γ_0 .

D. Nonreciprocal routing with normal mechanical modes

Under the strong coupling condition $J_m \gg \gamma$, we can introduce the normal modes (b_{\pm}) of the two coupled mechanical modes (b_1 and b_2) as

$$\delta b_{\pm} = \frac{1}{\sqrt{2}} (\delta b_1 \pm \delta b_2), \quad (28)$$

with resonant frequency $\omega_{\pm} = \omega_m \pm J_m$. The resonant frequency of ω_{\pm} provide us a clue to understand the scattering probabilities $S_{ij}(\omega)$ change dramatically round the splitting frequencies $\omega_m \pm J_m$.

The linearized QLEs (13) for the system can be rewritten with normal mechanical modes (b_{\pm}) as

$$\frac{d}{dt} V'(t) = -M'V'(t) + \sqrt{\Gamma_e}V'_{\text{in}}(t) + \sqrt{\Gamma_0}V'_{\text{noise}}(t), \quad (29)$$

$$\begin{aligned} V'(t) &\equiv (\delta a_1, \delta a_2, \delta b_+, \delta b_-)^T, \\ V'_{\text{in}}(t) &= (a_{1,\text{in}}, a_{2,\text{in}}, b_{+,\text{in}}, b_{-,\text{in}})^T, \quad V'_{\text{noise}}(t) = \\ &= (a_{1,\text{vac}}, a_{2,\text{vac}}, b_{+,\text{th}}, b_{-,\text{th}})^T, \text{ and} \end{aligned}$$

$$M' = \begin{pmatrix} \frac{\kappa}{2} + i\Delta_1 & iJ_c & i\frac{G_1 e^{i\phi_1}}{\sqrt{2}} & i\frac{G_1 e^{i\phi_1}}{\sqrt{2}} \\ iJ_c & \frac{\kappa}{2} + i\Delta_2 & i\frac{G_2 e^{i\phi_2}}{\sqrt{2}} & -i\frac{G_2 e^{i\phi_2}}{\sqrt{2}} \\ i\frac{G_1 e^{-i\phi_1}}{\sqrt{2}} & i\frac{G_2 e^{-i\phi_2}}{\sqrt{2}} & \frac{\gamma}{2} + i\omega_+ & 0 \\ i\frac{G_1 e^{-i\phi_1}}{\sqrt{2}} & -i\frac{G_2 e^{-i\phi_2}}{\sqrt{2}} & 0 & \frac{\gamma}{2} + i\omega_- \end{pmatrix}, \quad (30)$$

where

$$\delta b_{\pm,\text{in}} = \frac{1}{\sqrt{2}} (b_{1,\text{in}} \pm b_{2,\text{in}}), \quad (31)$$

$$\delta b_{\pm,\text{th}} = \frac{1}{\sqrt{2}} (b_{1,\text{th}} \pm b_{2,\text{th}}). \quad (32)$$

The scattering probabilities $S_{ij}(\omega)$ between modes j and i ($i, j = 1, 2, +, -$, for a_1, a_2, b_+, b_-) can be obtained follow the standard method as shown in the last paragraph of subsection II A.

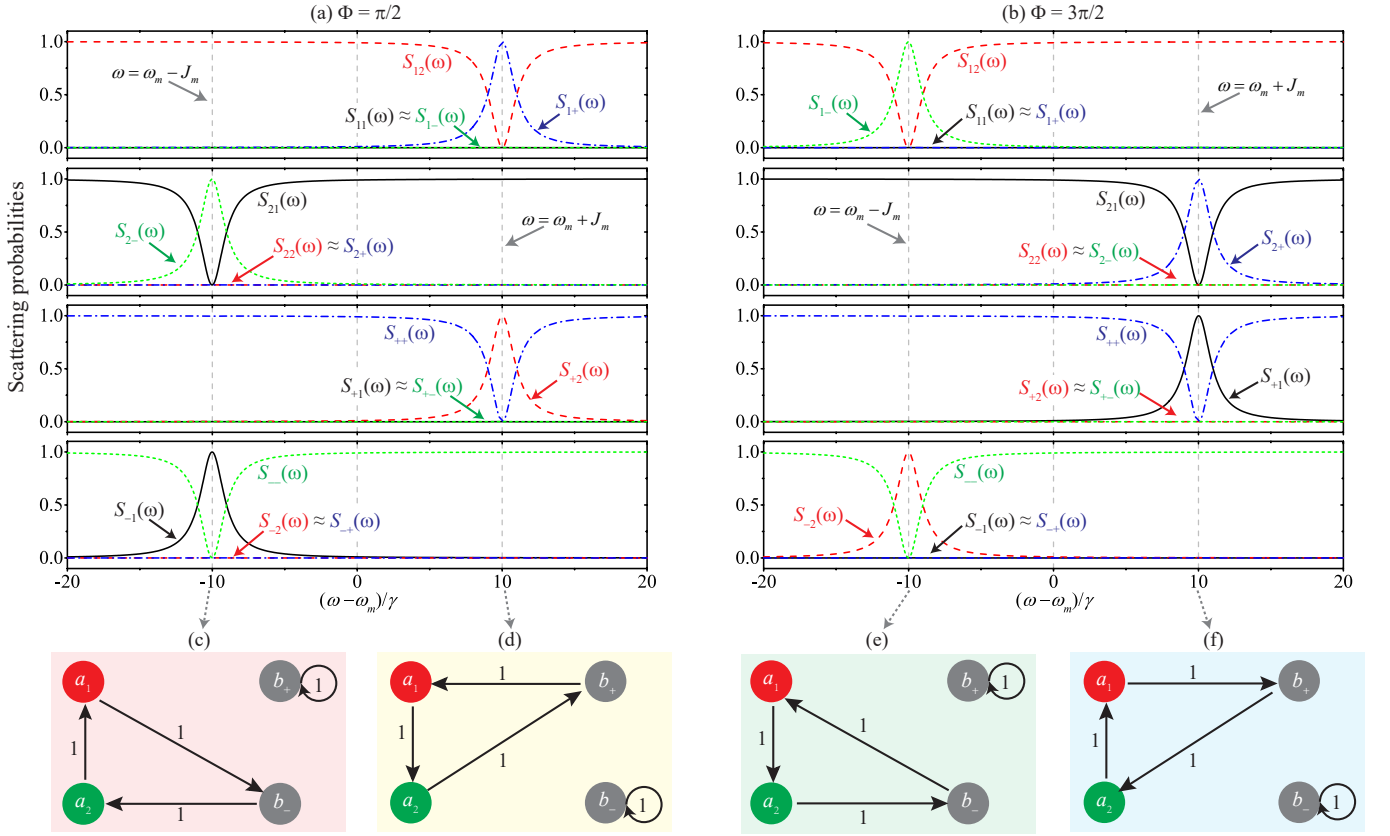


FIG. 5. (Color online) Scattering probabilities between different modes $S_{ij}(\omega)$ ($i, j = 1, 2, +, -$) versus frequency $(\omega - \omega_m)/\gamma$ for (a) $\Phi = \pi/2$ and (b) $\Phi = 3\pi/2$, with the corresponding probability flow charts shown in (c)-(f). The parameters are $\omega_1 = \omega_2 = \omega_m$, $\Delta_1 = \Delta_2 = \omega_m$, $J_m = 10\gamma$, $J_c = 500\gamma$, $\gamma_0 = \kappa_0 = 0$, $\gamma_e = \gamma$, $\kappa_e = \kappa$, $G_1 = G_2 = \sqrt{J_c\gamma}$, and $\kappa = 2J_c$.

The scattering probabilities $S_{ij}(\omega)$ between different modes are shown as functions of the frequency $(\omega - \omega_m)/\gamma$ in Fig. 5 for (a) $\Phi = \pi/2$ and (b) $\Phi = 3\pi/2$. We have $S_{++}(\omega) \approx 1$ and $S_{+1}(\omega) \approx S_{+2}(\omega) \approx S_{+-}(\omega) \approx 0$ for $\omega = \omega_m - J_m$. This means that the mechanical mode b_+ is decoupled from the system for large detuning, and only mechanical mode b_- is coupled to the two optical modes for resonant photon transport. Similarly, we have $S_{--}(\omega) \approx 1$ and $S_{-1}(\omega) \approx S_{-2}(\omega) \approx S_{-+}(\omega) \approx 0$ for $\omega = \omega_m + J_m$. That is to say the mechanical mode b_- is decoupled from the system for large detuning, and only mechanical mode b_+ is coupled to the two optical modes resonantly.

The probability flow charts are shown in Figs. 5(c)-5(f) for $\omega = \omega_m \pm J_m$ and $\Phi = \pi/2$ or $\Phi = 3\pi/2$. It is clear that we can realize nonreciprocal routing with optical mode a_1 as transmitter, a_2 as receiver, and the normal mechanical modes b_{\pm} as two terminals, as shown in Figs. 5(c) and 5(f). We can also realize nonreciprocal routing with a_1 as receiver, a_2 as transmitter, and the normal mechanical modes b_{\pm} as two terminals [see Figs. 5(d) and 5(e)]. Different from the proposal based on mechanical modes b_1 and b_2 shown in Fig. 2, where the signals are transport to b_1 and b_2 simultaneously, we can transport signals to only one of the terminal (b_+ or

b_-) with the other one decoupled from the optical modes. Moreover, the signals can transport between the two mechanical modes b_1 and b_2 with 25 percent probability, while there is no phonon transport between the normal mechanical modes (b_{\pm}).

IV. CONCLUSIONS

In summary, we have introduced a nonreciprocal router composing of a transmitter, a receiver, and two terminals, and the scattering probabilities are nonreciprocal. We have also proposed a scheme to realize the nonreciprocal router based on an optomechanical plaquette consisting of two optical and two mechanical modes, with one optical mode as transmitter, one optical mode as receiver, and two mechanical modes as terminals. We demonstrated that the transport direction of the signals in the router can be steered by the synthetic flux induced by the external driving fields, and the frequency of the input signals. We shew that the nonreciprocal router based on optomechanical plaquette are robust against the experimental imperfectness and within the reach of current experimental conditions. Our work lays the foundation for useful applications of nonreciprocal routers in quan-

tum network and quantum secure communication.

Province (Grant No. 2022RC1203).

Acknowledgement

This work is supported by the National Natural Science Foundation of China (Grants No. 12064010 and No. 12247105), Natural Science Foundation of Hunan Province of China (Grant No. 2021JJ20036), and the Science and Technology Innovation Program of Hunan

Appendix: Analytical expressions of the elements in scattering matrix

The elements of the matrix $U(\omega)$ in Eq. (20) are given by

$$U_{11}(\omega) = \frac{\kappa_e}{Z} \left\{ \left[\left(\frac{\gamma}{2} + i\omega_1 - i\omega \right) \left(\frac{\gamma}{2} + i\omega_2 - i\omega \right) + J_m^2 \right] \left(\frac{\kappa}{2} + i\Delta_2 - i\omega \right) + G_2^2 \left(\frac{\gamma}{2} + i\Delta_1 - i\omega \right) \right\} - 1, \quad (\text{A.1})$$

$$U_{12}(\omega) = -\frac{\kappa_e}{Z} \left[iJ_c \left(\frac{\gamma}{2} + i\omega_1 - i\omega \right) \left(\frac{\gamma}{2} + i\omega_2 - i\omega \right) - iJ_m G_1 G_2 e^{i(\phi_1 - \phi_2)} + iJ_c J_m^2 \right], \quad (\text{A.2})$$

$$U_{13}(\omega) = \frac{\sqrt{\kappa_e \gamma_e}}{Z} \left[-iG_2^2 G_1 e^{i\phi_1} + iJ_m J_c G_2 e^{i\phi_2} - iG_1 e^{i\phi_1} \left(\frac{\kappa}{2} + i\Delta_2 - i\omega \right) \left(\frac{\gamma}{2} + i\omega_2 - i\omega \right) \right], \quad (\text{A.3})$$

$$U_{14}(\omega) = -\frac{\sqrt{\kappa_e \gamma_e}}{Z} \left[J_c G_2 e^{i\phi_2} \left(\frac{\gamma}{2} + i\omega_1 - i\omega \right) + J_m G_1 e^{i\phi_1} \left(\frac{\kappa}{2} + i\Delta_2 - i\omega \right) \right], \quad (\text{A.4})$$

$$U_{21}(\omega) = -\frac{\kappa_e}{Z} \left[iJ_c \left(\frac{\gamma}{2} + i\omega_1 - i\omega \right) \left(\frac{\gamma}{2} + i\omega_2 - i\omega \right) - iJ_m G_1 G_2 e^{-i(\phi_1 - \phi_2)} + iJ_c J_m^2 \right], \quad (\text{A.5})$$

$$U_{22}(\omega) = \frac{\kappa_e}{Z} \left\{ \left[\left(\frac{\gamma}{2} + i\omega_1 - i\omega \right) \left(\frac{\gamma}{2} + i\omega_2 - i\omega \right) + J_m^2 \right] \left(\frac{\kappa}{2} + i\Delta_1 - i\omega \right) + G_1^2 \left(\frac{\gamma}{2} + i\omega_2 - i\omega \right) \right\} - 1, \quad (\text{A.6})$$

$$U_{23}(\omega) = -\frac{\sqrt{\kappa_e \gamma_e}}{Z} \left[J_m G_2 e^{i\phi_2} \left(\frac{\kappa}{2} + i\Delta_1 - i\omega \right) + J_c G_1 e^{i\phi_1} \left(\frac{\gamma}{2} + i\omega_2 - i\omega \right) \right], \quad (\text{A.7})$$

$$U_{24}(\omega) = \frac{\sqrt{\kappa_e \gamma_e}}{Z} \left[-iG_2 G_1^2 e^{i\phi_2} + iJ_c J_m G_1 e^{i\phi_1} - iG_2 e^{i\phi_2} \left(\frac{\kappa}{2} + i\Delta_1 - i\omega \right) \left(\frac{\gamma}{2} + i\omega_1 - i\omega \right) \right], \quad (\text{A.8})$$

$$U_{31}(\omega) = \frac{\sqrt{\kappa_e \gamma_e}}{Z} \left[-iG_2^2 G_1 e^{-i\phi_1} + iJ_c J_m G_2 e^{-i\phi_2} - iG_1 e^{-i\phi_1} \left(\frac{\kappa}{2} + i\Delta_2 - i\omega \right) \left(\frac{\gamma}{2} + i\omega_2 - i\omega \right) \right], \quad (\text{A.9})$$

$$U_{32}(\omega) = -\frac{\sqrt{\kappa_e \gamma_e}}{Z} \left[J_m G_2 e^{-i\phi_2} \left(\frac{\kappa}{2} + i\Delta_1 - i\omega \right) + J_c G_1 e^{-i\phi_1} \left(\frac{\gamma}{2} + i\Delta_2 - i\omega \right) \right], \quad (\text{A.10})$$

$$U_{33}(\omega) = \frac{\gamma_e}{Z} \left\{ \left[\left(\frac{\kappa}{2} + i\Delta_1 - i\omega \right) \left(\frac{\kappa}{2} + i\Delta_2 - i\omega \right) + J_c^2 \right] \left(\frac{\gamma}{2} + i\omega_2 - i\omega \right) + G_2^2 \left(\frac{\kappa}{2} + i\Delta_1 - i\omega \right) \right\} - 1, \quad (\text{A.11})$$

$$U_{34}(\omega) = -\frac{\gamma_e}{Z} \left[iJ_m \left(\frac{\kappa}{2} + i\Delta_1 - i\omega \right) \left(\frac{\kappa}{2} + i\Delta_2 - i\omega \right) - iJ_c G_1 G_2 e^{-i(\phi_1 - \phi_2)} + iJ_c^2 J_m \right], \quad (\text{A.12})$$

$$U_{41}(\omega) = -\frac{\sqrt{\kappa_e \gamma_e}}{Z} \left[J_c G_2 e^{-i\phi_2} \left(\frac{\gamma}{2} + i\omega_1 - i\omega \right) + J_m G_1 e^{-i\phi_1} \left(\frac{\kappa}{2} + i\Delta_2 - i\omega \right) \right], \quad (\text{A.13})$$

$$U_{42}(\omega) = \frac{\sqrt{\kappa_e \gamma_e}}{Z} \left[-iG_2 e^{-i\phi_2} \left(\frac{\kappa}{2} + i\Delta_1 - i\omega \right) \left(\frac{\gamma}{2} + i\omega_1 - i\omega \right) + iJ_c J_m G_1 e^{-i\phi_1} - iG_1^2 G_2 e^{-i\phi_2} \right], \quad (\text{A.14})$$

$$U_{43}(\omega) = -\frac{\gamma_e}{Z} \left[iJ_m \left(\frac{\kappa}{2} + i\Delta_1 - i\omega \right) \left(\frac{\kappa}{2} + i\Delta_2 - i\omega \right) - iG_1 G_2 J_c e^{i(\phi_1 - \phi_2)} + iJ_c^2 J_m \right], \quad (\text{A.15})$$

$$U_{44}(\omega) = \frac{\gamma_e}{Z} \left\{ \left[\left(\frac{\kappa}{2} + i\Delta_1 - i\omega \right) \left(\frac{\kappa}{2} + i\Delta_2 - i\omega \right) + J_c^2 \right] \left(\frac{\gamma}{2} + i\omega_1 - i\omega \right) + G_1^2 \left(\frac{\kappa}{2} + i\Delta_2 - i\omega \right) \right\} - 1, \quad (\text{A.16})$$

and

$$\begin{aligned} Z = & \left(\frac{\kappa}{2} + i\Delta_1 - i\omega \right) \left(\frac{\kappa}{2} + i\Delta_2 - i\omega \right) \left(\frac{\gamma}{2} + i\omega_1 - i\omega \right) \left(\frac{\gamma}{2} + i\omega_2 - i\omega \right) \\ & + G_1^2 \left(\frac{\kappa}{2} + i\Delta_2 - i\omega \right) \left(\frac{\gamma}{2} + i\omega_2 - i\omega \right) + G_2^2 \left(\frac{\kappa}{2} + i\Delta_1 - i\omega \right) \left(\frac{\gamma}{2} + i\omega_1 - i\omega \right) \\ & + J_c^2 \left(\frac{\gamma}{2} + i\omega_1 - i\omega \right) \left(\frac{\gamma}{2} + i\omega_2 - i\omega \right) + J_m^2 \left(\frac{\kappa}{2} + i\Delta_1 - i\omega \right) \left(\frac{\kappa}{2} + i\Delta_2 - i\omega \right) \\ & + J_c^2 J_m^2 + G_1^2 G_2^2 - 2J_c J_m G_1 G_2 \cos(\phi_1 - \phi_2). \end{aligned} \quad (\text{A.17})$$

-
- [1] M. Born and E. Wolf, *Principles of optics : electromagnetic theory of propagation, interference and diffraction of light*, 7th ed. (Cambridge University Press, 1999).
- [2] R. J. Potton, Reciprocity in optics, *Rep. Prog. Phys.* **67**, 717 (2004).
- [3] D. Jalas, A. Petrov, M. Eich, W. Freude, S. Fan, Z. Yu, R. Baets, M. Popović, A. Melloni, J. D. Joannopoulos, M. Vanwolleghem, C. R. Doerr, and H. Renner, What is – and what is not – an optical isolator, *Nat. Photonics* **7**, 579 (2013).
- [4] C. Caloz, A. Alù, S. Tretyakov, D. Sounas, K. Achouri, and Z.-L. Deck-Léger, Electromagnetic nonreciprocity, *Phys. Rev. Appl.* **10**, 047001 (2018).
- [5] M. Aspelmeier, T. J. Kippenberg, and F. Marquardt, Cavity optomechanics, *Rev. Mod. Phys.* **86**, 1391 (2014).
- [6] E. Verhagen and A. Alù, Optomechanical nonreciprocity, *Nat. Phys.* **13**, 922 (2017).
- [7] S. Barzanjeh, A. Xuereb, S. Gröblacher, M. Paternostro, C. A. Regal, and E. M. Weig, Optomechanics for quantum technologies, *Nat. Phys.* **18**, 15 (2022).
- [8] S. Manipatruni, J. T. Robinson, and M. Lipson, Optical nonreciprocity in optomechanical structures, *Phys. Rev. Lett.* **102**, 213903 (2009).
- [9] Z. Wang, L. Shi, Y. Liu, X. Xu, and X. Zhang, Optical Nonreciprocity in Asymmetric Optomechanical Couplers, *Sci. Rep.* **5**, 8657 (2015).
- [10] X.-W. Xu, L. N. Song, Q. Zheng, Z. H. Wang, and Y. Li, Optomechanically induced nonreciprocity in a three-mode optomechanical system, *Phys. Rev. A* **98**, 063845 (2018).
- [11] L. N. Song, Q. Zheng, X.-W. Xu, C. Jiang, and Y. Li, Optimal unidirectional amplification induced by optical gain in optomechanical systems, *Phys. Rev. A* **100**, 043835 (2019).
- [12] M. Hafezi and P. Rabl, Optomechanically induced nonreciprocity in microring resonators, *Opt. Express* **20**, 7672 (2012).
- [13] Z. Shen, Y.-L. Zhang, Y. Chen, F.-W. Sun, X.-B. Zou, G.-C. Guo, C.-L. Zou, and C.-H. Dong, Reconfigurable optomechanical circulator and directional amplifier, *Nat. Commun.* **9**, 1797 (2018).
- [14] F. Ruesink, J. P. Mathew, M.-A. Miri, A. Alù, and E. Verhagen, Optical circulation in a multimode optomechanical resonator, *Nat. Commun.* **9**, 1798 (2018).
- [15] Z. Shen, Y.-L. Zhang, Y. Chen, C.-L. Zou, Y.-F. Xiao, X.-B. Zou, F.-W. Sun, G.-C. Guo, and C.-H. Dong, Experimental realization of optomechanically induced nonreciprocity, *Nat. Photonics* **10**, 657 (2016).
- [16] F. Ruesink, M.-A. Miri, A. Alù, and E. Verhagen, Nonreciprocity and magnetic-free isolation based on optomechanical interactions, *Nat. Commun.* **7**, 13662 (2016).
- [17] X. Xu, Y. Zhao, H. Wang, H. Jing, and A. Chen, Quantum nonreciprocity in quadratic optomechanics, *Photon. Res.* **8**, 143 (2020).
- [18] Z.-X. Tang and X.-W. Xu, Thermal-noise cancellation for optomechanically induced nonreciprocity in a whispering-gallery-mode microresonator, *Phys. Rev. Appl.* **19**, 034093 (2023).
- [19] C.-H. Dong, Z. Shen, C.-L. Zou, Y.-L. Zhang, W. Fu, and G.-C. Guo, Brillouin-scattering-induced transparency and non-reciprocal light storage, *Nat. Commun.* **6**, 6193 (2015).
- [20] J. Kim, M. C. Kuzyk, K. Han, H. Wang, and G. Bahl, Non-reciprocal Brillouin scattering induced transparency, *Nat. Phys.* **11**, 275 (2015).
- [21] H. Xu, D. Mason, L. Jiang, and J. G. E. Harris, Topological energy transfer in an optomechanical system with exceptional points, *Nature (London)* **537**, 80 (2016).
- [22] J.-Q. Zhang, J.-X. Liu, H.-L. Zhang, Z.-R. Gong, S. Zhang, L.-L. Yan, S.-L. Su, H. Jing, and M. Feng, Topological optomechanical amplifier in synthetic PT-symmetry, *Nanophotonics* **11**, 721 (2022).
- [23] D. Long, X. Mao, G.-Q. Qin, H. Zhang, M. Wang, G.-Q. Li, and G.-L. Long, Dynamical encircling of the exceptional point in a largely detuned multimode optomechanical system, *Phys. Rev. A* **106**, 053515 (2022).
- [24] B. Li, R. Huang, X. Xu, A. Miranowicz, and H. Jing, Nonreciprocal unconventional photon blockade in a spinning optomechanical system, *Photon. Res.* **7**, 630 (2019).
- [25] Y.-F. Jiao, S.-D. Zhang, Y.-L. Zhang, A. Miranowicz, L.-M. Kuang, and H. Jing, Nonreciprocal optomechanical entanglement against backscattering losses, *Phys. Rev. Lett.* **125**, 143605 (2020).
- [26] W.-A. Li, G.-Y. Huang, J.-P. Chen, and Y. Chen, Nonreciprocal enhancement of optomechanical second-order sidebands in a spinning resonator, *Phys. Rev. A* **102**, 033526 (2020).
- [27] B. Li, i. m. c. K. Özdemir, X.-W. Xu, L. Zhang, L.-M. Kuang, and H. Jing, Nonreciprocal optical solitons in a spinning kerr resonator, *Phys. Rev. A* **103**, 053522 (2021).
- [28] D.-W. Zhang, L.-L. Zheng, C. You, C.-S. Hu, Y. Wu, and X.-Y. Lü, Nonreciprocal chaos in a spinning optomechanical resonator, *Phys. Rev. A* **104**, 033522 (2021).
- [29] Y.-F. Jiao, J.-X. Liu, Y. Li, R. Yang, L.-M. Kuang, and H. Jing, Nonreciprocal enhancement of remote entanglement between nonidentical mechanical oscillators, *Phys. Rev. Appl.* **18**, 064008 (2022).
- [30] M. Peng, H. Zhang, Q. Zhang, T.-X. Lu, I. M. Mirza, and H. Jing, Nonreciprocal slow or fast light in anti- \mathcal{PT} -symmetric optomechanics, *Phys. Rev. A* **107**, 033507 (2023).
- [31] X. Shang, H. Xie, G. Lin, and X. Lin, Nonreciprocity Steered with a Spinning Resonator, *Photonics* **9**, 585 (2022).
- [32] M. Schmidt, S. Kessler, V. Peano, O. Painter, and F. Marquardt, Optomechanical creation of magnetic fields for photons on a lattice, *Optica* **2**, 635 (2015).
- [33] A. Metelmann and A. A. Clerk, Nonreciprocal photon transmission and amplification via reservoir engineering, *Phys. Rev. X* **5**, 021025 (2015).
- [34] X.-W. Xu and Y. Li, Optical nonreciprocity and optomechanical circulator in three-mode optomechanical systems, *Phys. Rev. A* **91**, 053854 (2015).
- [35] L. Tian and Z. Li, Nonreciprocal quantum-state conversion between microwave and optical photons, *Phys. Rev. A* **96**, 013808 (2017).
- [36] M.-A. Miri, F. Ruesink, E. Verhagen, and A. Alù, Optical nonreciprocity based on optomechanical coupling, *Phys. Rev. Appl.* **7**, 064014 (2017).
- [37] X.-W. Xu, Y. Li, B. Li, H. Jing, and A.-X. Chen, Nonreciprocity via nonlinearity and synthetic magnetism,

- Phys. Rev. Applied* **13**, 044070 (2020).
- [38] X.-B. Yan, H.-L. Lu, F. Gao, and L. Yang, Perfect optical nonreciprocity in a double-cavity optomechanical system, *Front. Phys.* **14**, 52601 (2019).
- [39] X.-W. Xu, Y. Li, A.-X. Chen, and Y.-x. Liu, Nonreciprocal conversion between microwave and optical photons in electro-optomechanical systems, *Phys. Rev. A* **93**, 023827 (2016).
- [40] Y. Li, Y. Y. Huang, X. Z. Zhang, and L. Tian, Optical directional amplification in a three-mode optomechanical system, *Opt. Express* **25**, 18907 (2017).
- [41] D. Malz, L. D. Tóth, N. R. Bernier, A. K. Feofanov, T. J. Kippenberg, and A. Nunnenkamp, Quantum-limited directional amplifiers with optomechanics, *Phys. Rev. Lett.* **120**, 023601 (2018).
- [42] C. Jiang, L. N. Song, and Y. Li, Directional amplifier in an optomechanical system with optical gain, *Phys. Rev. A* **97**, 053812 (2018).
- [43] Y.-T. Lan, W.-J. Su, H. Wu, Y. Li, and S.-B. Zheng, Nonreciprocal light transmission via optomechanical parametric interactions, *Opt. Lett.* **47**, 1182 (2022).
- [44] S. J. M. Habraken, K. Stannigel, M. D. Lukin, P. Zoller, and P. Rabl, Continuous mode cooling and phonon routers for phononic quantum networks, *New J. Phys.* **14**, 115004 (2012).
- [45] H. Xu, L. Jiang, A. A. Clerk, and J. G. E. Harris, Nonreciprocal control and cooling of phonon modes in an optomechanical system, *Nature (London)* **568**, 65 (2019).
- [46] D.-G. Lai, J.-F. Huang, X.-L. Yin, B.-P. Hou, W. Li, D. Vitali, F. Nori, and J.-Q. Liao, Nonreciprocal ground-state cooling of multiple mechanical resonators, *Phys. Rev. A* **102**, 011502 (2020).
- [47] J.-X. Liu, Y.-F. Jiao, Y. Li, X.-W. Xu, Q.-Y. He, and H. Jing, Phase-controlled asymmetric optomechanical entanglement against optical backscattering, *Sci. China Phys. Mech. Astron.* **66**, 230312 (2023).
- [48] A. Seif, W. DeGottardi, K. Esfarjani, and M. Hafezi, Thermal management and non-reciprocal control of phonon flow via optomechanics, *Nat. Commun.* **9**, 1207 (2018).
- [49] Z. Denis, A. Biella, I. Favero, and C. Ciuti, Permanent directional heat currents in lattices of optomechanical resonators, *Phys. Rev. Lett.* **124**, 083601 (2020).
- [50] S. Barzanjeh, M. Aquilina, and A. Xuereb, Manipulating the flow of thermal noise in quantum devices, *Phys. Rev. Lett.* **120**, 060601 (2018).
- [51] M. Schmidt, V. Peano, and F. Marquardt, Optomechanical Dirac physics, *New J. Phys.* **17**, 023025 (2015).
- [52] V. Peano, C. Brendel, M. Schmidt, and F. Marquardt, Topological Phases of Sound and Light, *Phys. Rev. X* **5**, 031011 (2015).
- [53] C. Sanavio, V. Peano, and A. Xuereb, Nonreciprocal topological phononics in optomechanical arrays, *Phys. Rev. B* **101**, 085108 (2020).
- [54] K. Fang, J. Luo, A. Metelmann, M. H. Matheny, F. Marquardt, A. A. Clerk, and O. Painter, Generalized nonreciprocity in an optomechanical circuit via synthetic magnetism and reservoir engineering, *Nat. Phys.* **13**, 465 (2017).
- [55] J. P. Mathew, J. d. Pino, and E. Verhagen, Synthetic gauge fields for phonon transport in a nano-optomechanical system, *Nat. Nanotechnol.* **15**, 198 (2020).
- [56] J. del Pino, J. J. Slim, and E. Verhagen, Non-Hermitian chiral phononics through optomechanically induced squeezing, *Nature (London)* **606**, 82 (2022).
- [57] Y. Chen, Y.-L. Zhang, Z. Shen, C.-L. Zou, G.-C. Guo, and C.-H. Dong, Synthetic gauge fields in a single optomechanical resonator, *Phys. Rev. Lett.* **126**, 123603 (2021).
- [58] G. A. Peterson, F. Lecocq, K. Cicak, R. W. Simmonds, J. Aumentado, and J. D. Teufel, Demonstration of efficient nonreciprocity in a microwave optomechanical circuit, *Phys. Rev. X* **7**, 031001 (2017).
- [59] N. R. Bernier, L. D. Tóth, A. Koottandavida, M. A. Ioannou, D. Malz, A. Nunnenkamp, A. K. Feofanov, and T. J. Kippenberg, Nonreciprocal reconfigurable microwave optomechanical circuit, *Nat. Commun.* **8**, 604 (2017).
- [60] S. Barzanjeh, M. Wulf, M. Peruzzo, M. Kalaei, P. B. Dieterle, O. Painter, and J. M. Fink, Mechanical on-chip microwave circulator, *Nat. Commun.* **8**, 953 (2017).
- [61] L. Mercier de Lépinay, E. Damskägg, C. F. Ockeloen-Korppi, and M. A. Sillanpää, Realization of directional amplification in a microwave optomechanical device, *Phys. Rev. Applied* **11**, 034027 (2019).
- [62] L. Mercier de Lépinay, C. F. Ockeloen-Korppi, D. Malz, and M. A. Sillanpää, Nonreciprocal transport based on cavity floquet modes in optomechanics, *Phys. Rev. Lett.* **125**, 023603 (2020).
- [63] X. Gu, A. F. Kockum, A. Miranowicz, Y. xi Liu, and F. Nori, Microwave photonics with superconducting quantum circuits, *Phys. Rep.* **718-719**, 1 (2017), microwave photonics with superconducting quantum circuits.
- [64] L. Zhou, L.-P. Yang, Y. Li, and C. P. Sun, Quantum routing of single photons with a cyclic three-level system, *Phys. Rev. Lett.* **111**, 103604 (2013).
- [65] J. Lu, L. Zhou, L.-M. Kuang, and F. Nori, Single-photon router: Coherent control of multichannel scattering for single photons with quantum interferences, *Phys. Rev. A* **89**, 013805 (2014).
- [66] C. Gonzalez-Ballester, E. Moreno, F. J. Garcia-Vidal, and A. Gonzalez-Tudela, Nonreciprocal few-photon routing schemes based on chiral waveguide-emitter couplings, *Phys. Rev. A* **94**, 063817 (2016).
- [67] D.-C. Yang, M.-T. Cheng, X.-S. Ma, J. Xu, C. Zhu, and X.-S. Huang, Phase-modulated single-photon router, *Phys. Rev. A* **98**, 063809 (2018).
- [68] J. Zhou, X.-L. Yin, and J.-Q. Liao, Chiral and nonreciprocal single-photon scattering in a chiral-giant-molecule waveguide-qed system, *Phys. Rev. A* **107**, 063703 (2023).
- [69] T. Aoki, A. S. Parkins, D. J. Alton, C. A. Regal, B. Dayan, E. Ostby, K. J. Vahala, and H. J. Kimble, Efficient routing of single photons by one atom and a microtoroidal cavity, *Phys. Rev. Lett.* **102**, 083601 (2009).
- [70] K. Xia and J. Twamley, All-optical switching and router via the direct quantum control of coupling between cavity modes, *Phys. Rev. X* **3**, 031013 (2013).
- [71] Y. T. Zhu and W. Z. Jia, Single-photon quantum router in the microwave regime utilizing double superconducting resonators with tunable coupling, *Phys. Rev. A* **99**, 063815 (2019).
- [72] Z. Wang, Y. Wu, Z. Bao, Y. Li, C. Ma, H. Wang, Y. Song, H. Zhang, and L. Duan, Experimental realization of a deterministic quantum router with superconducting quantum circuits, *Phys. Rev. Appl.* **15**, 014049 (2021).
- [73] G. S. Agarwal and S. Huang, Optomechanical systems as single-photon routers, *Phys. Rev. A* **85**, 021801 (2012).

- [74] X. Li, W.-Z. Zhang, B. Xiong, and L. Zhou, Single-photon multi-ports router based on the coupled cavity optomechanical system, *Sci. Rep.* **6**, 39343 (2016).
- [75] X.-W. Xu, A.-X. Chen, Y. Li, and Y.-x. Liu, Nonreciprocal single-photon frequency converter via multiple semi-infinite coupled-resonator waveguides, *Phys. Rev. A* **96**, 053853 (2017).
- [76] I.-C. Hoi, C. M. Wilson, G. Johansson, T. Palomaki, B. Peropadre, and P. Delsing, Demonstration of a single-photon router in the microwave regime, *Phys. Rev. Lett.* **107**, 073601 (2011).
- [77] J.-N. Wu, J. Dong, Y. Xu, B. Zou, and Y. Zhang, Multichannel adjustable single-photon router based on large detuning, *Phys. Rev. Appl.* **18**, 054007 (2022).
- [78] W.-B. Yan and H. Fan, Single-photon quantum router with multiple output ports, *Sci. Rep.* **4**, 4820 (2014).
- [79] G. Li, X. Xiao, Y. Li, and X. Wang, Tunable optical nonreciprocity and a phonon-photon router in an optomechanical system with coupled mechanical and optical modes, *Phys. Rev. A* **97**, 023801 (2018).
- [80] L. Du, Y.-T. Chen, J.-H. Wu, and Y. Li, Nonreciprocal interference and coherent photon routing in a three-port optomechanical system, *Opt. Express* **28**, 3647 (2020).
- [81] A. Metelmann and H. E. Türeci, Nonreciprocal signal routing in an active quantum network, *Phys. Rev. A* **97**, 043833 (2018).
- [82] Y.-l. Ren, S.-l. Ma, J.-k. Xie, X.-k. Li, M.-t. Cao, and F.-l. Li, Nonreciprocal single-photon quantum router, *Phys. Rev. A* **105**, 013711 (2022).
- [83] Z. Shen, Y.-L. Zhang, Y. Chen, Y.-F. Xiao, C.-L. Zou, G.-C. Guo, and C.-H. Dong, Nonreciprocal frequency conversion and mode routing in a microresonator, *Phys. Rev. Lett.* **130**, 013601 (2023).
- [84] C. W. Gardiner and M. J. Collett, Input and output in damped quantum systems: Quantum stochastic differential equations and the master equation, *Phys. Rev. A* **31**, 3761 (1985).
- [85] R. Burgwal and E. Verhagen, Enhanced nonlinear optomechanics in a coupled-mode photonic crystal device, *Nat. Commun.* **14**, 1526 (2023).